Los Alamos
NATIONAL LABORATORY
EST. 1943

LA-UR-16-22677
Approved for public release; distribution is unlimited.

Title: MCNP and GADRAS Comparisons

Author(s): Klasky, Marc Louis
Myers, Steven Charles
James, Michael R.
Mayo, Douglas R.

Intended for: Report

Issued: 2016-04-19

Disclaimer:
Los Alamos National Laboratory, an affirmative action/equal opportunity employer,is operated by the Los Alamos National Security, LLC for the National NuclearSecurity Administration of the U.S. Department of Energy under contract DE-AC52-06NA25396. By approving this article, the publisher recognizes that the U.S. Government retains nonexclusive, royalty-free license to publish or reproduce the published form of this contribution, or to allow others to do so, for U.S. Government purposes. Los Alamos National Laboratory requests that the publisher identify this article as work performed under the auspices of the U.S. Departmentof Energy. Los Alamos National Laboratory strongly supports academic freedom and a researcher's right to publish; as an institution, however, the Laboratory does not endorse the viewpoint of a publication or guarantee its technical correctness.

MCNP and GADRAS Comparisons

Los Alamos National Laboratory

April 12, 2016

Work Performed by:

Marc Klasky, Steve Myers, Michael James, Doug Mayo

Contents

1.0 Background

To facilitate the timely execution of System Threat Reviews (STRs) for DNDO, and also to develop a methodology for performing STRs, LANL performed comparisons of several radiation transport codes (MCNP[1], GADRAS[2], and Gamma-Designer[3]) that have been previously utilized to compute radiation signatures. While each of these codes has strengths, it is of paramount interest to determine the limitations of each of the respective codes and to also identify the most time efficient means by which to produce computational results given the large number of parametric cases that are anticipated in performing STR's. These comparisons serve to identify regions of applicability for each code and provide estimates of uncertainty that may be anticipated. Furthermore, while performing these comparisons, examination of the sensitivity of the results to modeling assumptions was also examined. These investigations serve to enable the creation of the LANL methodology for performing STRs.

Given the wide variety of radiation test sources, scenarios, and detectors, LANL calculated comparisons of the following parameters: decay data, multiplicity, device (n,γ) leakages, and radiation transport through representative scenes and shielding. This investigation was performed to understand potential limitations utilizing specific codes for different aspects of the STR challenges. In this manner LANL will develop an independent methodology for each of the necessary steps for performing STR work and, along with LLNL, understand the consistency of results between the two laboratories.

2.0 Activities

The following tasks were performed to examine code differences and areas of applicability of computational methods.

1. Comparisons of Decay line data for selected materials (GADRAS /MISC[4])
2. Comparisons of Source Aging Pu and HEU (GADRAS , MISC)
3. Comparison of multiplicity of radiation test sources (MCNP/GADRAS/ Gamma-Designer)
4. Comparison of (n,γ) leakages from 1-D unshielded radiation test sources (using different forms of SNM and also reflector materials) (MCNP,GADRAS, Gamma-Designer)
5. Comparisons of radiation transport from 1D radiation test sources through shielding to detectors (MCNP/GADRAS/ Gamma-Designer)
6. Examination of the Human Portable Tripwire (HPT) STR[5] and comparisons to the LLNL baseline scenario results
7. Comparisons of neutron and photon leakages using GADRAS/MCNP/ Gamma-Designer for objects in the Threat Matrix

This report will report the results of Tasks 1-6. An additional report will be written to describe the results of Tasks 7.

3.0 Tasks 1-2 Results

A comparison of the fundamental data utilized in both the neutron and photon intrinsic radiation calculations was examined using both the MISC code and GADRAS. In addition, a comparison of the build-in of Am-241 using GADRAS, the LANL NEN-1 code FRAM[6], as well as the LANL code Decayculator [7](developed by NEN-2) was performed. The results of this investigation are presented in Table 1. Specifically, the bold values for each code represent the ratio of the 5, 20, and 40 year results to the 1 year values. As may be observed from examination of Table 1 the results are consistent between the three independent codes. Minor differences in those ratios are the result of minor differences in the assumed half-lives of Pu-241 and Am-241.

Code/Parameter	1 year age	5 year age	20 year age	40 year age
GADRAS/662 keV flux	3.80E+04	1.72E+05	4.90E+05	6.60E+05
Ratio to 1 year value	1.0	**4.532**	**12.885**	**17.367**
FRAM/Mass percent	0.02355	0.10695	0.30515	0.41244
Ratio to 1 year value	1.0	**4.541**	**12.958**	**17.513**
Decayculator/mCi activity	1.6	7.1	20.2	27.3
Ratio to 1 year value	1.0	**4.438**	**12.625**	**17.063**

Table 1 Comparisons of GADRAS Calculated Am-241 Ingrowth with Age

Comparisons of the fundamental decay data were also performed by first comparing the decay lines of Pu-239 and U-235 using both GADRAS and the MISC code. These comparisons were performed for a number of specified aging scenarios, namely 0, 10, 20, and 40 years. For Plutonium-239 comparisons of the largest intensity lines indicate excellent agreement i.e. 0.995 in the ratio of the intensities with the exceptions listed in Table 2. Comparison of the intensities for uranium-235 indicates even better agreement generally 1 with the exceptions listed in Table 3.

Energy Kev	Ratio MISC/GADRAS
13.6	1.06
16.4	1.19
98.4	2
103	1.06
111	2
112	.076
116	1.06

Table 2 Comparison of Pu-239 Decay Lines

Energy Kev	Ratio Intensity GADRAS/MISC
93.8	1.15
82.1*	1.03
58.6*	0.96

* Th-231 Line

Table 3 Comparison of U-235 Decay Lines

It should be noted that in general these ratios were independent of the aging period examined.

In addition to the comparison of the photon decay lines an investigation was performed to compare the spontaneous fission rates. This comparison was performed using MCNP and GADRAS. The results of this investigation are presented in Table 4.

Isotope	MCNP Spontaneous Fission Rate n/(sec gram)	GADRAS Spontaneous Fission Rate n/(sec gram)
U232	1.3	0
U233	$8.6x10^{-4}$	$3.79x10^{-4}$
U234	$5.02x10^{-3}$	$6.86x10^{-3}$
U235	$2.99x10^{-4}$	$1.04x10^{-5}$
U236	$5.49x10^{-3}$	$4.28x10-^{3}$
U238	$1.36x10^{-2}$	$1.35x10^{-2}$
Pu238	$2.59x10^{3}$	$2.64x10^{3}$
Pu239	$2.18x10^{-2}$	$1.51x10^{-2}$
Pu240	$1.02x10^{3}$	$1.05x10^{3}$
Pu241	$5x10^{-2}$	$2.03x10^{-3}$
Pu242	$1.72x10^{3}$	$1.74x10^{3}$

Table 4 Comparisons of Spontaneous Fission Rates

4.0 Tasks 3-4 Results

A series of one-dimensional radiation test sources was constructed utilizing both GADRAS and MCNP to compare the neutron and photon transport results. These tests objects contained both uranium and plutonium with a variety of isotopics in both metal and oxide forms. The test suite also utilized varying degrees of reflection with both depleted uranium as well as polyurethane (PE). Examples of bare, uranium reflected, as well as a uranium/PE reflected object are presented in Figures 1-3 respectively. Comparisons of neutron leakages were performed with MCNP using both the isotopics as determined by GADRAS as well as the MCNP built in spontaneous fission (SF) source. (It should be noted that in the case in which the MCNP source

is utilized only the principle components are utilized i.e. no age neutron emission is present.) Finally, the effect of steel shielding was examined. Details on the isotopics utilized as well as the age for each of the respective cases are provided in Appendix A.

Table 5 provides the comparisons of the k_{eff}, and neutron and photon leakages for 54 configurations. (Compositions for Materials utilized in Table 5 are defined in Appendix A.) The analysis of these results is presented in Sections 6-8.

Table 5 Benchmark Cases

Case #	Material Composition	SNM Mass (kg)	Density g/cm^3	Reflector	GADRAS k_{eff}	MCNP k_{eff}	GADRAS Gamma Leakage	MCNP Gamma Leakage	GADRAS Neutron Leakage	MCNP Neutron Leakage (Run only with SF source)
1	Pu[i]	4.22	15. 75	Bare	0.664	.662	$5.3x10^8$	5.1x108	$4.37x10^5$	$4.28x10^5$
2	Pu[i]	8.25	15.75	Bare	0.809	.811	$8.28x10^8$	$8.28x10^8$	$1.39 x10^6$	$1.37x10^6$
3	Pu[i]	14.25	15.75	Bare	0.951	.954	$1.2x10^9$	$1.189x10^9$	$8.47 x10^6$	$8.72x10^6$
4	Pu[i]	15.72	15.75	Bare	0.978	.983	$1.28x10^9$	$1.273x10^9$	$2.1 x10^7$	$2.41x10^7$
5	Pu[i]	16.5	15.75	Bare	0.992	.996	$1.34x10^9$	$1.316x10^9$	$6.05 x10^7$	XX
6	Pu[i]	4.22	15.75	DU[ii] 1cm	0.722	.725	$1.12x10^6$	$1.09x10^6$	$5.32x10^5$	$5.24x10^5$
7	Pu[i]	4.22	15.75	DU[ii] 2 cm	0.761	0.764	$1.37 x10^6$	$1.346x10^6$	$6.16 x10^5$	$6.07x10^5$
8	Pu[i]	4.22	15.75	DU[ii] 3 cm	0.789	0.793	$1.8 x10^6$	$1.77x10^6$	$6.93 x10^5$	$6.868x10^5$
9	Pu-239 96% Pu-240 4% Zero age	2.83	15.75	1 cm U238 and 15.45 cm PE[iii]	.772	.8006	$6.74x10^5$	$5.55x10^5$	$3.6x10^4$	3.05x104
10	Pu-239 96% Pu-240 4% Zero age	2.83	15.75	1 cm U238 and 35.45 cm PE[iii]	.774	.8015	$2.06x10^5$	$1.36x10^5$	671	819
11	Pu-239 96% Pu-240 4% Zero age	2.83	15.75	1 cm U238 and 55.45 cm PE[iii]	.774	.8012	$5.74x10^4$	$2.7x10^4$	43.9	37
14	HEU[iv]	7.48	18.95	2 cm DU and 33.45 PE[iii]	0.755	0.785	$1.87x10^5$	$2.04x10^5$	0.687	.758
15	HEU[iv]	13.57	18.95	2 cm DU and 33.45 PE[iii]	.886	0.916	$2.43x10^5$	$2.5x10^5$	2.11	2.11
16	HEU[iv]	21.3	18.95	2 cm DU and 33.45 PE[iii]	0.992	1.036	$2.83x10^5$	XX	14.5	XX
17	HEU[iv]	7.48	18.95	2 cm DU[ii]	0.643	.664	$1.53x10^6$	$1.58x10^6$	$2.91x10^2$	292
18	HEU[iv]	21.3	18.95	2 cm DU[ii]	0.874	0.9	$2.55x10^6$	$2.54x10^6$	955	1070
19	HEU Oxide[v]	45.91	10.96	2 cm DU[ii] and 33.45cm PE[iii]	0.984	1.01	$5.72x10^5$	$5.7x10^5$	71.6	XX
20	HEU Oxide[v]	100.53	3	2 cm DU[ii] and 55.45 cm PE[iii]	0.748	0.822	$1.59x10^6$	$1.56x10^6$	15	17.8
21	PU Oxide[vi]	73.29	3	2 cm DU[ii] and 33.45 cm PE[iii]	0.932	1.00	$1.47x10^7$	XX	$1.38x10^5$	XX
22	Pu Oxide[vi]	86.19	3	2 cm DU and 33.45 cm PE***	0.967	1.038	$3.03x10^7$	XX	$1.77x10^5$	XX
23	Pu Oxide[vi]	73.29	3	2 cm DU[ii]	0.715	0.717	$1.63x10^7$	$1.57x10^7$	$1.67x10^7$	$7.93x10^6$
24	Pu[i] (thin shell 0.01 thicknessRi-46.2 cm)	4.23	15.75	Bare			$6.4x10^{10}$	$6.462x10^1$	$2.5x10^5$	$1.95x10^5$
25	Pu[i] (Ri=14.57 0.1	4.23	15.75	Bare			$7.3x10^9$	$7.028x10^9$	$2.08x10^5$	$1.99x10^5$

	thick)									
26	Pu[i] (Ri=6.29 0.5 thick)	4.23	15.75	Bare			$1.52x10^{9}$	$1.529x10^{9}$	$2.43x10^{5}$	$2.04x10^{5}$
28	PuO_2 [vi] (Ri 441.4 0.01 thick)	73.45	3	Bare			$3.68x10^{12}$	$3.759x10^{1}$	$6.29x10^{6}$	$3x10^{6}$
29	Pu O_2 [vi] (Ri 139.527	73.45	3	Bare			$6.09x10^{11}$	$6.154x10^{1}$	$6.33x10^{6}$	$3.02x10^{6}$
30	Pu O_2 (Ri 62.1704)	73.45	3	Bare			$1.28x10^{10}$	$1.280x10^{1}$	$6.53x10^{6}$	$3.14x10^{6}$
31	HEU[iv] (thin shell Ri=56.1 thickness 0.01)	7.5	18.95	Bare			$4.35x10^{8}$	$4.336x10^{8}$	6.05	8.05
32	HEU[iv] thin shell Ri=17.6918 thickness 0.1)	7.5	18.95	Bare			$7.72x10^{7}$	$7.5X10^{7}$	6.19	8.18
33	HEU[iv] thin shell Ri=7.68306 thickness 0.5)	7.5	18.95	Bare			$1.65x10^{7}$	$1.620x10^{7}$	6.77	8.27
45	U-235	5.08	18.95	Bare	0.504	.504	$4.02x10^{6}$	$3.99x10^{6}$	.0814	2.33
46	U-235	17.15	18.95	Bare	0.743	0.744	$9.05x10^{6}$	$8.914x10^{6}$	0.443	12.75
47	U-235	40.64	18.95	Bare	0.959	.959	$1.61x10^{7}$	$1.588x10^{7}$	5.32	154.5
52	Pu240	0.07 grams	15.75	Bare			$4.28x10^{5}$	$4.622x10^{5}$	69.4	6.788E+01
54	Pu-240	65.97grams	15.75	Bare			$4.32x10^{7}$	$4.661x10^{7}$	$7.53x10^{4}$	$7.39x10^{4}$
55	Pu-240	527.79 grams	15.75	Bare			$1.73x10^{8}$	$1.874x10^{8}$	$6.65x10^{5}$	$6.51x10^{5}$
57	Pu-240	4.22	15.75	Bare	0.487	.484	$6.94x10^{8}$	$7.518x10^{8}$	$6.92x10^{6}$	$6.74x10^{6}$
58	Pu-240	14.25	15.75	Bare	0.693	0.689	$1.57x10^{9}$	$1.70x10^{9}$	$3.45x10^{7}$	$3.34x10^{7}$
60	Pu238	4.22	15.75	Bare	0.659	0.698	$4.67x10^{10}$	$4.640x10^{1}$	$2.03x10^{7}$	$2.64x10^{7}$
61	Pu241	4.22	15.75	Bare	0.567	0.616	$2.06x10^{11}$	$2.196x10^{1}$	5810	4419
62	Pu242	4.22	15.75	Bare	0.401	0.398	$1x10^{7}$	$1.085x10^{7}$	$1.03x10^{7}$	$1.01x10^{7}$
64	Pu241	0.07 grams	15.75	Bare			$1.28x10^{8}$	$1.364x10^{8}$	$1.34x10^{-4}$	$3.3x10^{-3}$
65	U235	0.08	18.95	Bare			$2.03x10^{3}$	$2.024x10^{3}$	$8.32x10^{-7}$	$2.39x10^{-5}$
66 zero age	U238	0.08	18.95	Bare			.63	.887	$1.08x10^{-3}$	$1.08x10^{-3}$
67 zero age	U234	0.08	18.95	Bare			$1.22x10^{4}$	$1.425x10^{4}$	$5.48x10^{-4}$	$4.01x10^{-4}$
68 zero age	U232	0.08	18.95	Bare			$5.99x10^{7}$	$6.826x10^{7}$	0	0.105

[xx] Could not be computed due to the fact that the MCNP calculation revealed the case was supercritical

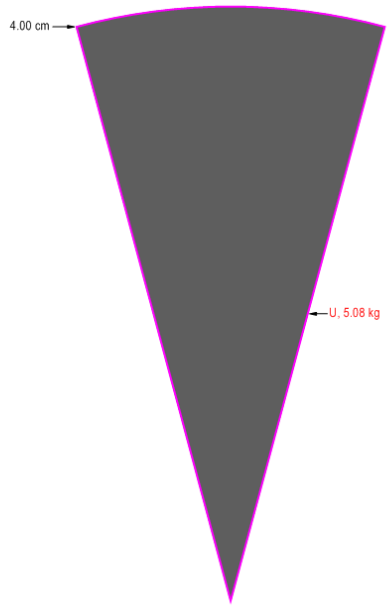

Figure 1 Representative One-Dimensional HEU Radiation Test Source

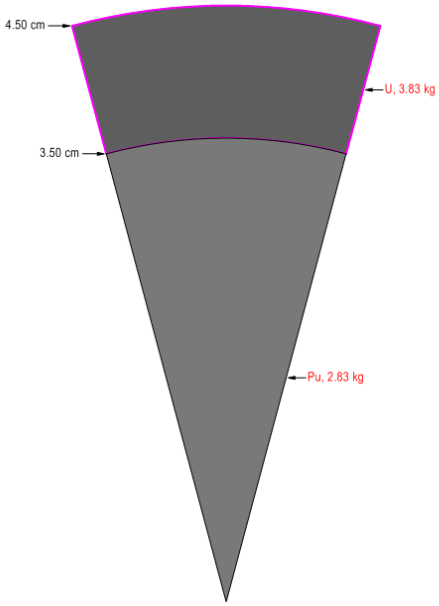

Figure 2 Representative One-Dimensional Plutonium-Uranium Reflected Test Source

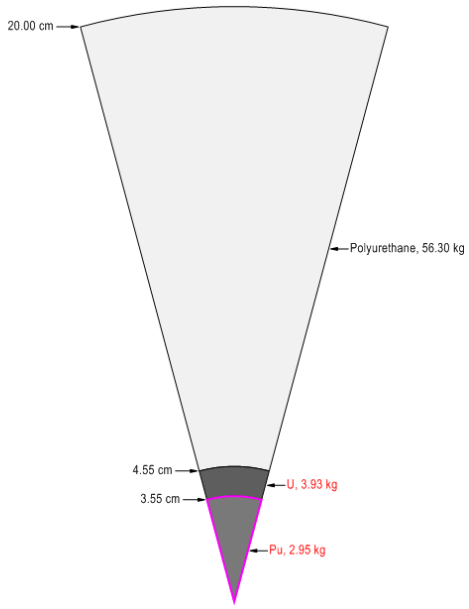

Figure 3 Representative One-Dimensional Plutonium-Uranium/PE Reflected Test Source

5.0 Analysis of the k_{eff} results

A comparison of the k_{eff} results using both GADRAS and MCNP is presented in **Figure 4** using a Histogram to indicate the number of cases having a specified deviation. The values on the x-axis in Figure 4 represent the result of subtracting the MCNP k_{eff} value from the GADRAS k_{eff} value i.e. Delta k. A difference of zero indicates exact agreement, while negative values indicate the GADRAS results were lower than the MCNP result, and positive values indicate GADRAS results were higher. The values on the y axis indicate the number of cases having a specified deviation.

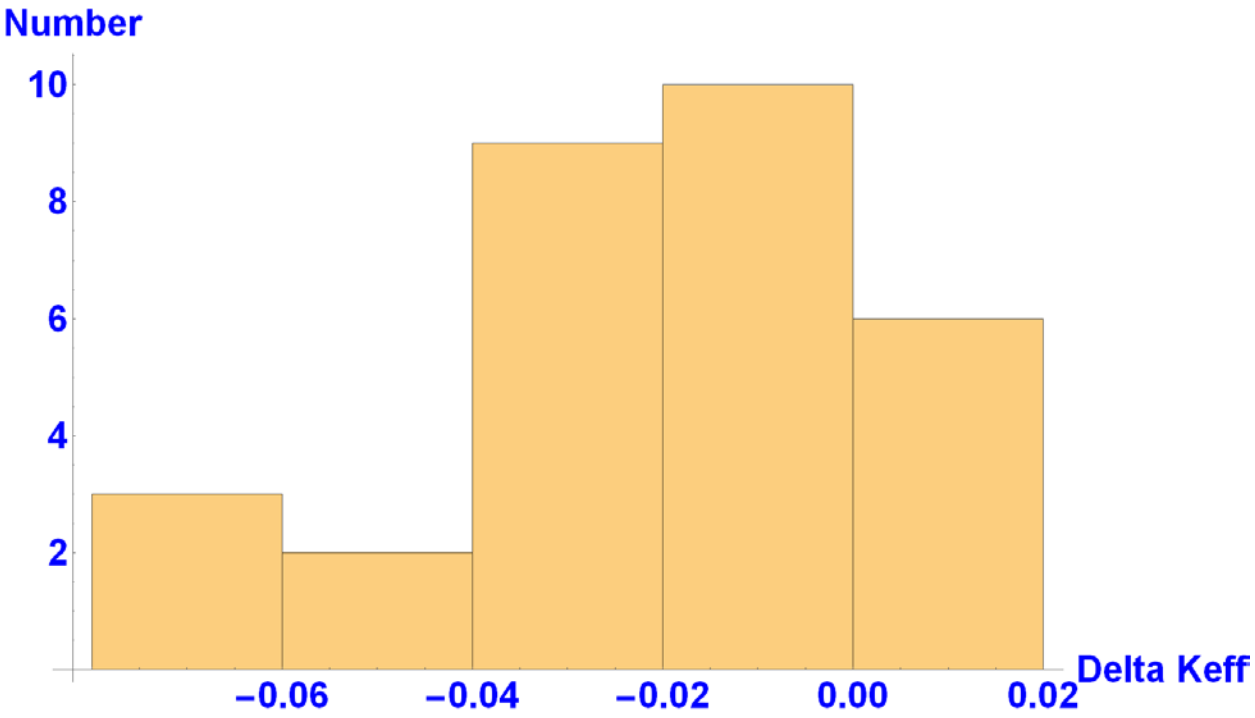

Figure 4 K_{eff} Difference (GADRAS minus MCNP) All Test sources

Examination of Figure 4 reveals an average bias of approximately -0.02 and a standard deviation of 0.0233 (The negative bias indicates that GADRAS tends to under predict k_{eff} relative to MCNP). However, a more detailed analysis of the data reveals that the bare HEU and Pu test sources, as may be observed from examination of Figures 5-6, have a much lower bias.

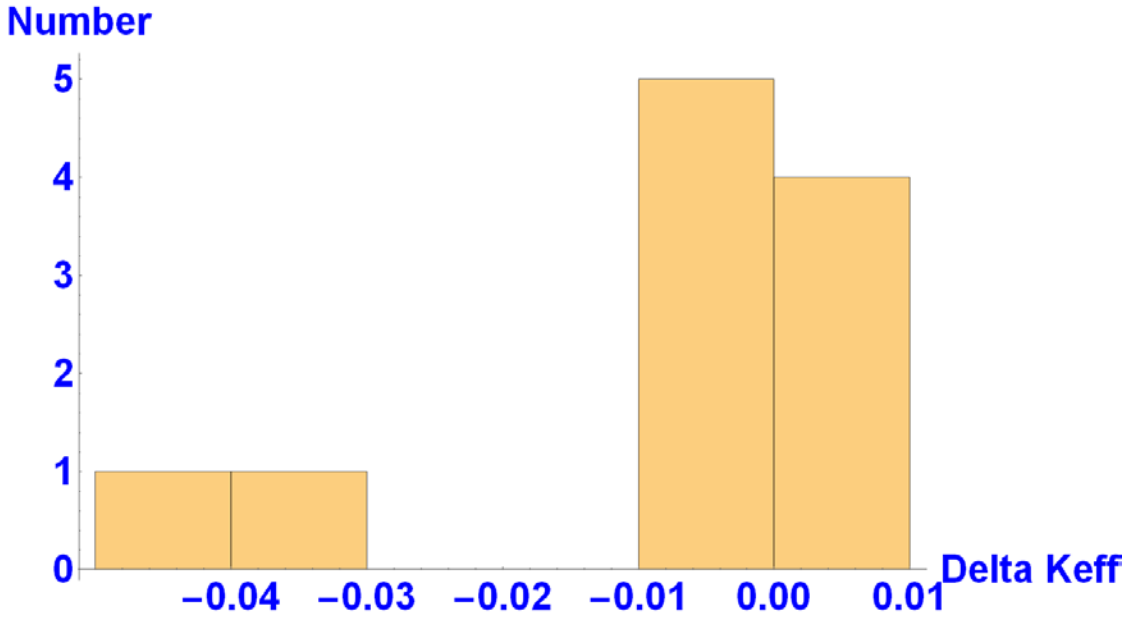

Figure 5 K_{eff} Difference (GADRAS minus MCNP) Pu Metal Bare Test sources

The average k_{eff} deviation was -0.0083 with a standard deviation of 0.0178 for bare Pu metal test sources.

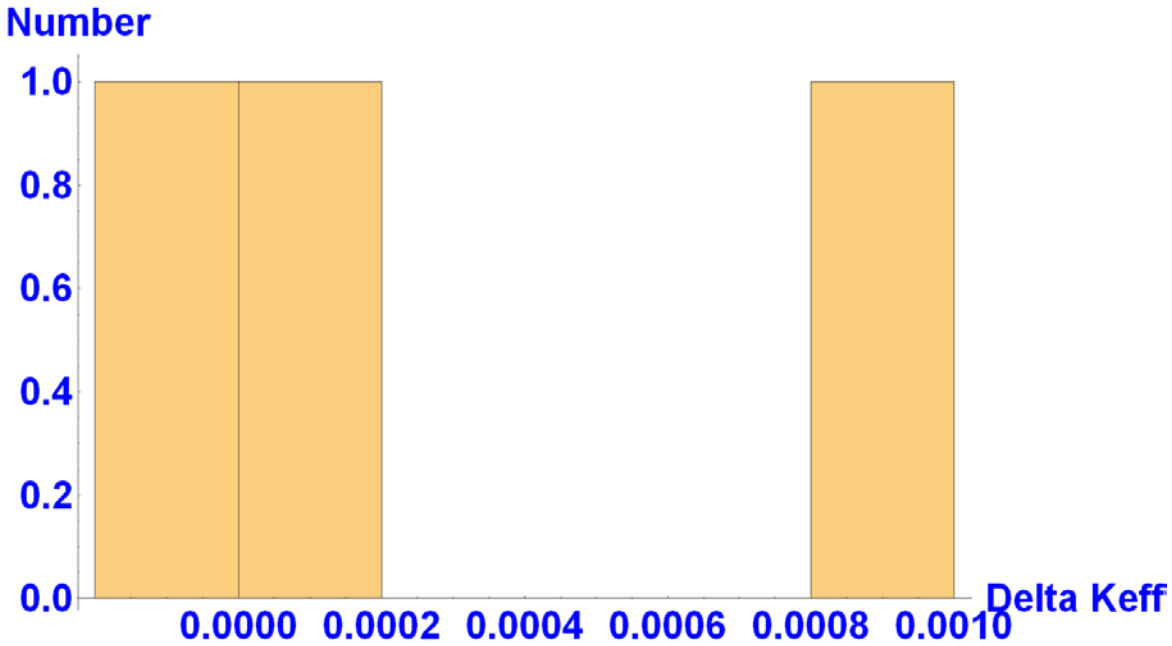

Figure 6 K_{eff} Difference (GADRAS minus MCNP) HEU Metal Bare Test sources

The average k_{eff} deviation was 0.0002 with a standard deviation of 0.00058 for bare HEU metal test sources.

The k_{eff} deviations for the uranium and plutonium reflected uranium test sources are presented in Figure 7.

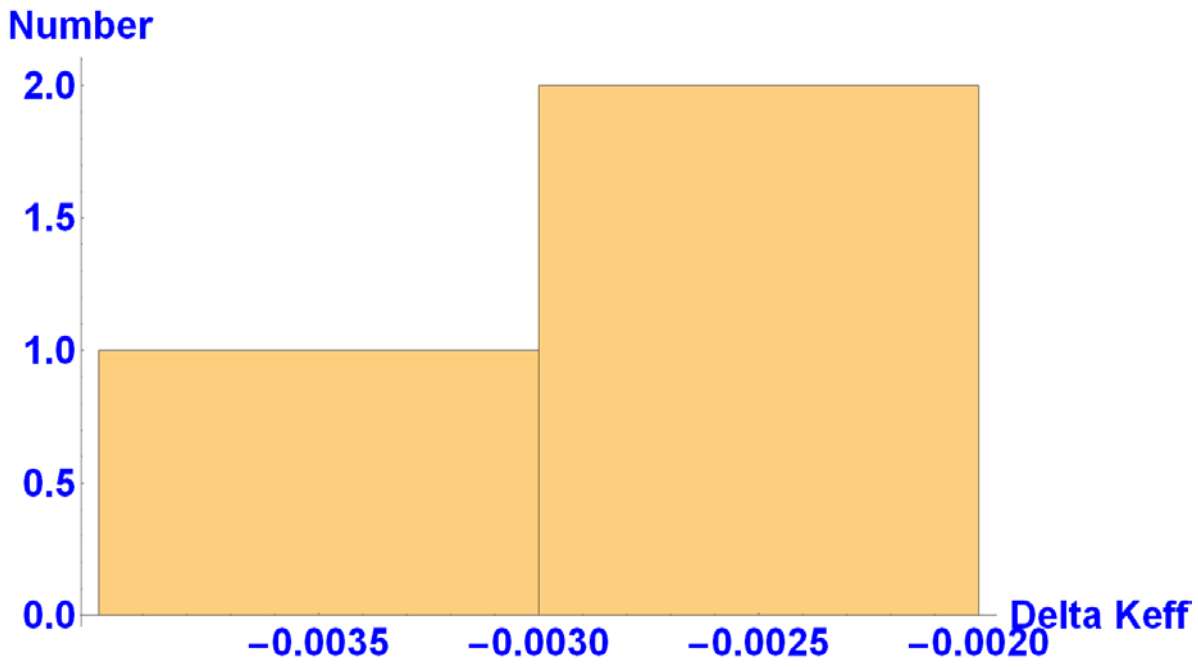

Figure 7 K_{eff} Difference (GADRAS minus MCNP) HEU/PU Uranium Reflected Test sources

The average k_{eff} deviation was -0.0033 with a standard deviation of 0.00057 for uranium reflected HEU/Pu test sources.

Finally, a comparison of the uranium and plutonium uranium/PE reflected, as depicted in Figure 3, is presented in Figure 8.

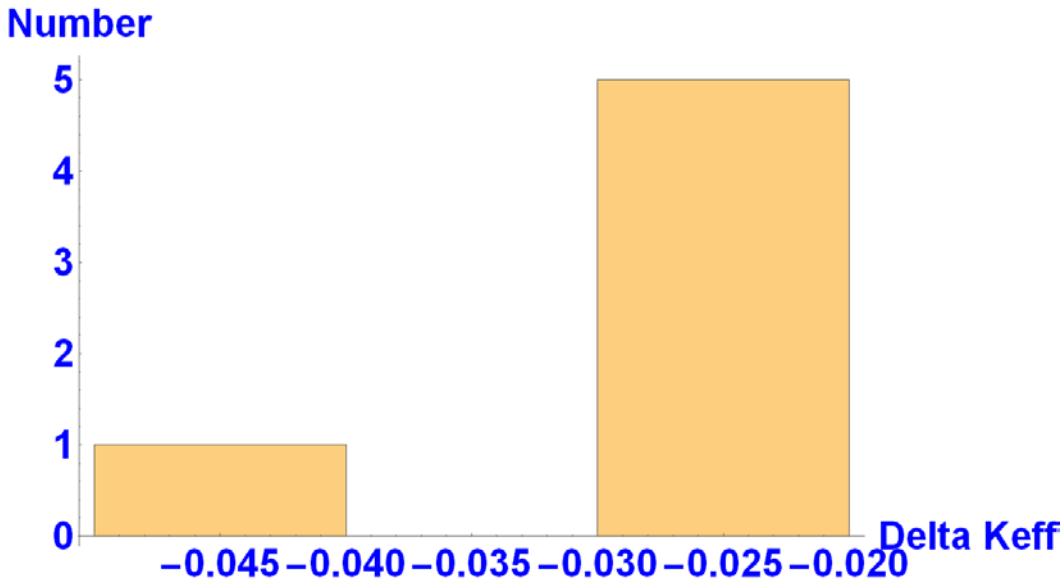

Figure 8 K_{eff} Difference (GADRAS minus MCNP) Pu/HEU Uranium/PE Reflected Test sources

As may be seen from examination of Figure 8, incorporation of PE results in a deviation of -0.03 with a standard deviation of 0.006. This sizeable deviation may lead to large deviations in the neutron multiplication and consequently the neutron leakages of test sources very close to critical. This may be seen by exploring the effect of a bias of 0.03 in the ratio of the neutron multiplications i.e. $(\frac{1-k_1}{1-k_2})$ where $k_2=k_1\pm0.03$. In Figure 9 we examine this ratio as a function of the reactivity of test source one, i.e. k_1

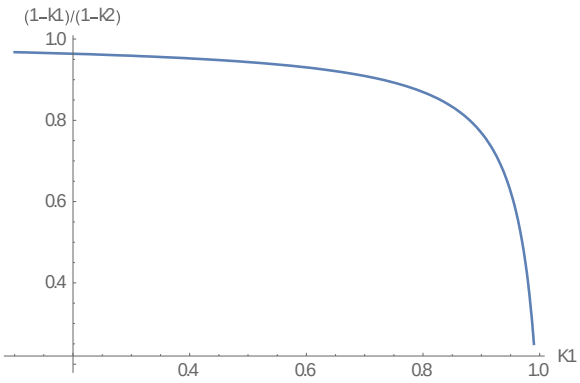

Figure 9 Ratio of Neutron Multiplications versus keff$_1$

As may be observed from examination of Figure 9 the ratio of the neutron multiplications decreases from an initial value of 0.97. The ratio becomes much larger than this initial value as the reactivity increases e.g. at a reactivity of 0.9 the ratio becomes 0.78. Accordingly, for test sources with neutron moderators it is recommended that MCNP be utilized in lieu of GADRAS for computing neutron leakages for test sources with reactivity in excess of 0.9.

6.0 Analysis of Neutron Leakages

A comparison of the neutron leakages obtain from the one-dimensional objects using both GADRAS and MCNP was performed. In general, the comparisons were performed using the SF source implemented in MCNP and the spontaneous fission rates that were implemented in GADRAS. However, in some cases to further explore the differences between the codes, MCNP was utilizing the neutron source generated by GADRAS. In this manner isolation of differences between spontaneous fission rates and differences in the neutron transport could be performed. Figure 10 presents a histogram of the ratios of the GADRAS/MCNP neutron leakages.

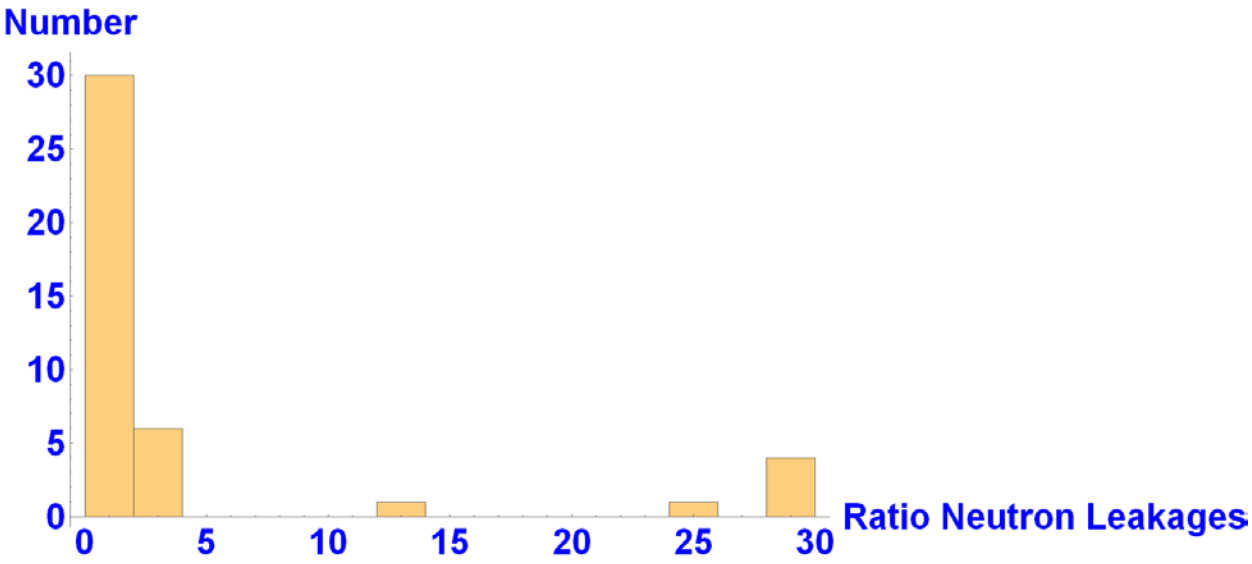

Figure 10 Histogram of Ratio (GADRAS/MCNP) Neutron Leakage All Cases

It should be noted that in assembling the histogram the larger of the ratio of GADRAS/MCNP or MCNP/GADRAS is presented. The average deviation of the ratio of neutron leakages using MCNP6 and GADRAS was determined to be 4.8 with a standard deviation of 8.9. As may be observed from examination of Figure 10, a large majority of the cases had relatively low differences (i.e. less than 20 percent) and the relatively high deviation is attributed to a few outliers. To resolve the outliers a detailed examination of these cases was performed.

For the plutonium oxide test sources a large discrepancy, factor of approximately two, was observed in the neutron leakages between GADRAS and MCNP when only the spontaneous fission source was included in the MCNP source definition and the α,n source was neglected. A subsequent investigation in which the GADRAS neutron source was utilized in MCNP was performed. In this manner the α,n source was included and deviations between GADRAS and MCNP were determined to be approximately 1%.

Finally, it was observed that the results containing the pure isotopes of U-235, Pu-241, U-232, and Pu-239 had significant differences in the GADRAS and MCNP results. The origin of these differences is the fundamental nuclear data. While MCNP utilizes the spontaneous fission rates from Ensslin [8], GADRAS utilizes ENDBF-VII[9]. When the same nuclear data is utilized in the transport calculation differences between GADRAS and MCNP are less than 1%.

For the plutonium test sources which contain even small amounts of Pu-240 the spontaneous fission rate of Pu-240 dominates the neutron production and consequently the significant differences in the Pu-239 and Pu-241 are not observed in all of the isotopic mixtures of plutonium in this study. Likewise, for the uranium test sources examined, even for HEU, the contribution of the U-238 spontaneous fission from U-238 minimizes the overall difference in the neutron production rates. Likewise, for U-233 test sources it is not envisioned that the small

impurity content of U-232 will lead to large deviations (GADRAS/MCNP) in the neutron leakages. Finally, when the GADRAS spontaneous fission rates are utilized in the MCNP calculations the deviations are observed to be less than 1%.

7.0 Analysis of photon leakages

Analysis of the comparison of the photon leakages of the GADRAS and MCNP objects turned out to be the more difficult. This was due to the fact that the comparison of the GADRAS results and MCNP must be made using the photon lines, the beta particle decay from aged U-238, and finally for test sources containing plutonium in conjunction with hydrogenous materials (n,γ). Furthermore, in some cases the absolute photon leakages are very sensitive to the lower energy limit specified for detection (e.g., 40 keV versus 10 keV).

Initial comparisons between GADRAS and MCNP in test sources containing DU had significant differences of at least a factor of two in most cases. However, the agreement significantly improved with the inclusion of the continuum radiation that is attributed to Pa234, Pa-234m, and Th-234. Finally, it was also found that in test sources in which Plutonium is present that it was necessary to include the capture radiation from the n,γ interaction in the hydrogen fraction of the PE.

Figure 11 presents a histogram depicting the differences for all cases.

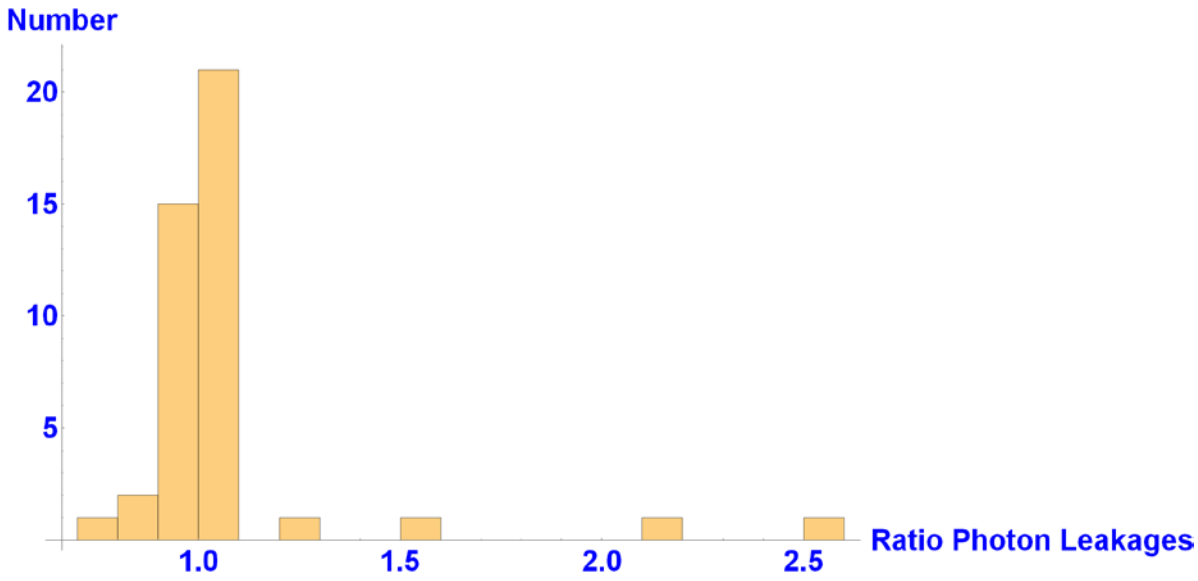

Figure 11 Histogram of Ratio (GADRAS/MCNP) Photon Leakage All Cases

The average deviation for these cases has been computed to be 1.05 with a standard deviation of 0.308. The outlier cases are cases in which plutonium is reflected by a relatively thick layer of

PE. This difference in the photon leakages may be attributed to the capture of neutrons in the hydrogen atoms of the PE.

8.0 One Dimensional Cases with Steel Shielding

An examination of the effect of a layer of Stainless steel outside of a one dimensional object was also investigated. The results of this investigation are presented in Table 6.

Material	Uranium Reflector Outer Radius	Fissile Mass Kg	PEouter radius	SS Thickness	Gamma leakage GADRAS	MCNP Gamma Leakage	Neutron leakage GADRAS	MCNP Neutron Leakage
U235	4	5.08	NA	0.5	$2.03x10^{6}$	$2.12058x10^{6}$	.0814	0.0816
U235	4	5.08	NA	2.54	$2.01x10^{5}$	$2.68940x10^{5}$	.0811	0.0814
U235	4	5.08	2 cm DU	2.54	$4.97x10^{5}$	$5.08x10^{5}$	214	214.9
Puo2 /1in SS	4	.804	6	2.54	$5.23x10^{5}$	$5.6x10^{5}$	$8.14x10^{4}$	$8.13796x10^{4}$
Puo2 /1in SS +PE30cm	4	.804	36	2.54	$1.62x10^{5}$	$1.87x10^{5}$	217	211 4.95680E+02
HEU /DU and 30 cm PE	4	5.08	36	2.54	$1.34x10^{5}$	$1.5x10^{4}$	.597	1.64

Table 6 Examination of Stainless Steel Shielding

9. HPT STR Examination

Members of the Los Alamos National Laboratory (LANL) system threat review (STR) team evaluated the capabilities of a subset of the Human Portable Tripwire (HPT) detection systems in an effort to compare our assessment to one that was previously performed by the Lawrence Livermore National Laboratory (LLNL) STR team. We used the Gamma Detection and Response Analysis Software (GADRAS) developed at Sandia National Laboratory to evaluate the following four HPT systems: Mirion 100 PDS, Polimaster PM 1704, the FLIR nanoRaider, and a notional CZT detector with dimensions of 1.0 cm depth by 3.6 cm height and 3.6 cm width. For the sake of expediency, two CsI detectors were not evaluated (the Polimaster 1703 and the D-Tect) as their response function characterization was not available in GADRAS and would need to be modeled. Furthermore, their performance is expected to be comparable to the other two CsI detectors that were evaluated in this effort (Mirion 100 PDS and Polimaster 1704) as they are of similar size and volume.

The baseline scenario was the only one evaluated and included these detection specifics:

- A user moving at a velocity of 2 ft/sec with the distance of closest approach equal to 1 meter
- A 1 second signal integration time upon which to evaluate detection

- A six sigma detection threshold, with sigma defined as the square root of the gross background counts expected in the detector during the one second integration time
- Background exposure rates as follows: 0.4 microR/hr over water (Water Low), 1 microR/hr over water (Water High), 5 microR/hr over land (Land Low), and 10 microR/hr over land (Land High)
- An additional shield of 0.4 cm of iron added to the models between the threat matrix items and the detectors

LANL used the same background rates and sigma values assumed for the gamma detectors that were postulated by LLNL to ensure a straightforward comparison. LANL performed calculations to integrate the change in gamma count rate of a moving detector and applied that correction to the 6 sigma detection threshold values. All threat matrix items were modeled in GADRAS using information provided by LLNL. However, one of those items was not modeled as the information provided to date is not sufficient to produce a viable model. In some cases there are minor differences in LANL models that were required in order to maintain consistency between masses, volumes and densities in different materials present in the threat designs. It is not anticipated these small differences will have a significant impact on the calculations of detectability.

The neutron detection capability of the HPT systems was not evaluated for two specific reasons. First, none of the HPT neutron detectors were characterized for GADRAS and, therefore, much more time consuming MCNP calculations would have been required. Secondly, the LLNL HPT report does not specify what threshold values they used for neutron detection. Thus, a straightforward comparison is not possible.

Table 7 presents the comparison of the difference in the total number of items LANL identified as detectable in the baseline scenario as compared to the total number predicted by LLNL. A negative value indicates that LANL predicted fewer items would be detectable than LLNL, and a positive number indicates the opposite. Finally, it is not possible to know which specific items in the threat matrix were considered undetectable by LLNL as that level of detail was not provided in their report. Therefore only this broad comparison can be made. As seen in Table 7, none of the differences are substantial given the total number of cases involved, and the deviations are somewhat balanced between positive and negative outcomes. Conclusions one would have drawn from the LANL evaluation are comparable to the ones drawn from the LLNL assessment.

Table 7. Differences in Totals Deemed Detectable Between LANL and LLNL Assessments

Detector	Water (Low)	Water (High)	Land (Low)	Land (High)
Mirion 100 PDS	0	4	-2	-7
FLIR nanoRaider	9	6	-2	1
Polimaster 1704	-6	-8	4	3
Notional CZT	4	3	2	6

10.0 Conclusions

A comprehensive examination of the neutron and photon calculations for one dimensional radiation test sources containing uranium and plutonium has been performed. Comparisons of the fundamental data as well as the neutron multiplicity as given by k_{eff} and the neutron and photon leakages have been presented. In general, excellent agreement between GADRAS and MCNP has been demonstrated. A negative bias in the k_{eff} of GADRAS relative to MCNP is observed in test sources containing hydrogenous materials. This bias is attributed to the use of a group cross section set that is collapsed with a weighting function for fast test sources. . Accordingly, for test sources with neutron moderators it is recommended that MCNP be utilized in lieu of GADRAS for computing neutron leakages for test sources with reactivity in excess of 0.9. Comparisons of the neutron leakages indicate excellent agreement within ~20% for all test sources with the exception of the oxides and pure quantities of Pu-239, U-235, U-232, and Pu-241. The MCNP neutron leakages in oxides are low by approximately a factor of two due to the absence of the (α,n) source.

Comparisons of the photon leakages indicate excellent agreement between MCNP and GADRAS except for cases in which a large quantify of moderating material surrounds the object. In these cases differences ranging from approximately 20% to a factor of two are indicated. These differences are attributed to differences in the production of photons via neutron capture reactions in the moderating material. Consequently, it is recommended that for cases in which the detectability is within a factor of two of a detection boundary that MCNP calculations be performed to validate the GADRAS results. Finally, we demonstrated a subset of HPT calculations that show the LANL conclusions on detection would not contradict the original conclusions reported by LLNL.

Appendix A

The composition of the materials used in benchmarking is provided below.

i Ga 0.6, Pu-236 9.94×10^{-9},Pu-238 1.49×10^{-2},Pu-239 94.7,Pu-240 4.47,Pu-241 0.15,Pu-242 2.98 Age 20 years

ii DU ρ=18.95 U-234 1.5×10^{-3} %, U-235 0.2 %, U-238 99.799 % Age 20 years

iii Polyurethane ρ=1.7 C 59%, H 6.7%, N 8%, O 26.3 %

iv HEU U-232 1×10^{-8}, U-234 0.5%, U-235 93.5, U-236 0.6 %, U-238 5.5% Age 20 years

v U-232 1.27×10^{-8}, U-234 0.5936, U-235 79.2, U-236 0.42 , U 238 4.49, O 15.2 Percentages Age 20 years

vi Pu-236 8.82×10^{-9}, Pu-238 1.32×10^{-2}, Pu-239 84.07, Pu-240 3.968, Pu-241 0.141, Pu-242 2.65×10^{-3} , O 11.802 Percentages Age 20 years

[11] Pelowitz, D.B., et al.," MCNP6™USER'S MANUAL Version 1.1," Los Alamos National Laboratory, LA-CP-14-00745, Rev. 0, June 2014
[2] GADRAS
[3] Gamma Designer,
[4] Solomon, Clell J. Jr.,MCNP Intrinsic Source Constructor (MISC): A User's Guide
[5] HPT STR
[6] Decayculator
[7] FRAM
[8] Ensslin, N. et al., "Application Guide to Neutron Multiplicity Counting," Los Alamos National Laboratory report LA-13422-M (November 1998).
[9] Nuclear Data SheetsVolume 112, Issue 12, Pages 2887-3152 (December 2011)Special Issue on ENDF/B- VII.1 Library Edited by Pavel Obložinský